



52nd SME North American Manufacturing Research Conference (NAMRC 52, 2024)

## In-process Part Tracking and Shape Measurement using Vision-based Motion Capture for Automated English Wheeling

Yahui Zhang, Derick Suarez, Kornel Ehmann, Jian Cao, Ping Guo\*

*Department of Mechanical Engineering, Northwestern University, Evanston, IL, 60208, USA*

\* Corresponding author. *E-mail address:* [ping.guo@northwestern.edu](mailto:ping.guo@northwestern.edu)

---

### Abstract

An English wheel is an exceedingly adaptable instrument in traditional metalworking. It is a manual manufacturing technique, enabling skilled craftsmen and blacksmiths to shape complex compound curves in sheet metal panels. Accurate measurements and precise adjustments are essential when operating an English wheel to ensure that the metal is shaped with the desired curvature. An automated method to form English wheeled panels through robot forming has recently been proposed. For such a method to be successful, accurate tracking of sheet information including positions, orientations, and deformation is important for error compensation and the design of the subsequent tool paths. In this study, a Vicon motion capture system is employed to monitor the position and shape of the sheet metal during the English wheeling process. The initial experimental results demonstrate the potential of such an in-process metrology system, along with possible avenues for future work.

© 2024 The Authors. Published by ELSEVIER Ltd. This is an open access article under the CC BY-NC-ND license

(<https://creativecommons.org/licenses/by-nc-nd/4.0>)

Peer-review under responsibility of the scientific committee of the NAMRI/SME.

*Keywords:* Metrology; Flexible Sheet Metal Forming Process; Automation; Computer vision; Motion Capture

---

### 1. Introduction

Metal forming continues to hold a dominant position within the manufacturing sector. As the demand for customized parts that can be produced grows, so does the need for increased flexibility. The goal is to achieve high productivity in crafting intricate shapes while adhering to strict tolerances in physical dimensions [1]. To cater to these evolving requirements, conventional metal forming tools like the hammer, English wheel, shrinker/stretcher, and spinning lathe have undergone renewed scrutiny and adaptation to align with current industry standards [2, 3, 4]. Due to its exceptional ability to shape intricate compound curves with precision, the English wheel stands out among these processes.

Accurate measurements and precise adjustments are essential when operating an English wheel to ensure that the metal sheet is shaped with the desired curvature. Traditionally, craftsmen use their eyes and tactile feedback as sensors for real-

time adjustments during the process, especially as large curvatures are imparted to the sheet. Recently, the use of robots to form sheet metal panels using the English wheel as a method to achieve repeatable results has been suggested [4]. For robotic forming to mimic the degree of accuracy of a traditional craftsman more closely, metrological components must be integrated.

Metrology plays a paramount role in the manufacturing processes, serving as the science of measurement and underpinning the foundation of quality assurance, precision, and accuracy. Its significance lies in its ability to guarantee that manufactured products align with design specifications and stringent quality standards, thereby meeting customer expectations and complying with regulatory requirements. Metrology also empowers manufacturers with real-time process control capabilities, allowing for constant monitoring and adjustments to maintain consistent product quality. Metrological systems not only contribute to the assurance of

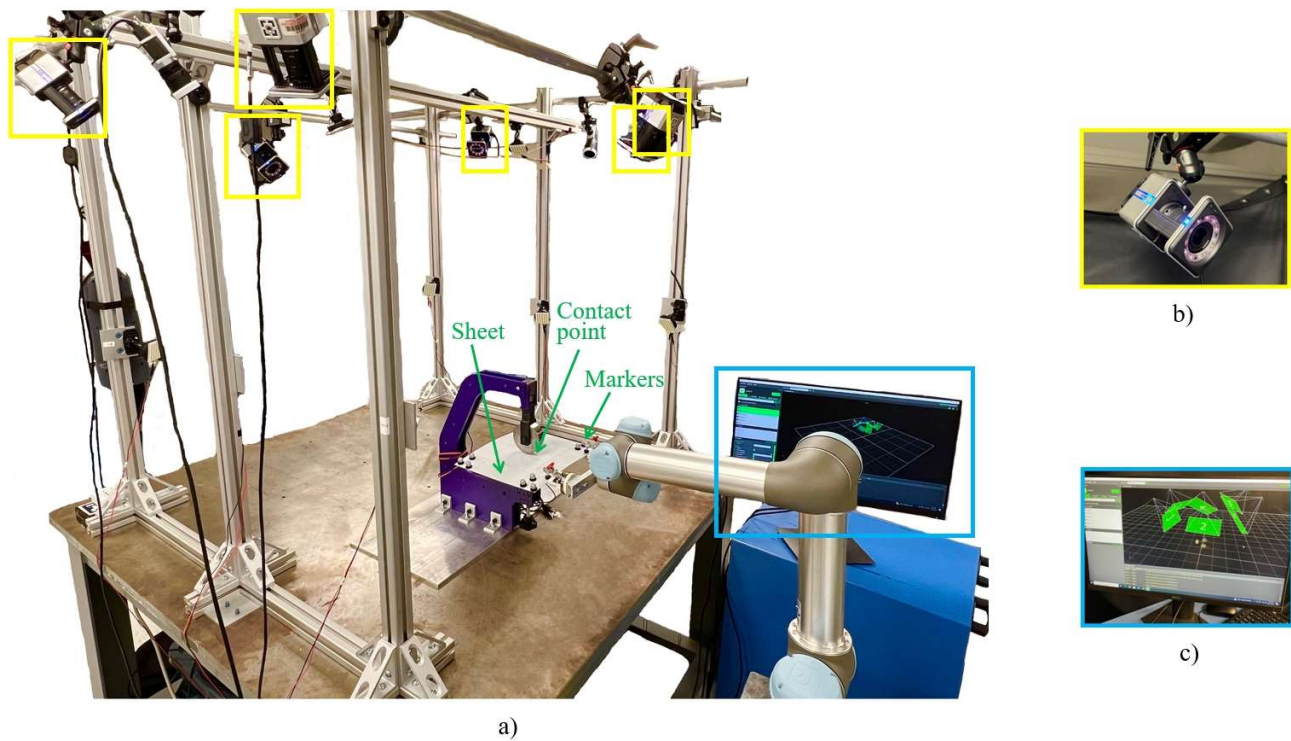


Figure 1. Experimental setup: a) overview of the entire system setup, b) the Vicon system consisting of six infrared cameras, and c) software to provide the 3D locations of markers attached to the object in real-time.

high-quality products but also result in cost reduction as early issue identification reduces the need for reworks. Some of the commonly used metrology techniques today include Coordinate Measuring Machines (CMMs) [5] equipped with touch probes or laser scanners, which allow precise 3D measurements of complex parts, optical and vision measurement systems [6, 7], which utilize advanced optics and cameras for non-contact measurements, 3D scanning technologies for capturing detailed surface information [8, 9], and portable metrology devices such as portable arms and laser trackers, enabling flexibility in on-site measurements [10, 11]. These techniques are employed across various industries, from aerospace and automotive to healthcare and electronics, ensuring quality control and precision in manufacturing and research but often carry high costs and have limited applicability in processes like English wheeling. Additionally, the use of advanced software for data analysis and visualization has become integral to modern metrology, enhancing the accuracy and efficiency of measurement processes [12, 13].

In this work, a motion capture system, Vicon, is employed to track the metal sheet's positions and shape during the English wheeling process. The Vicon system is a cutting-edge motion capture solution designed to capture and analyze human and animal movements. These systems have revolutionized the fields of biomechanics, animation, sports analysis, and more. Vicon technology uses infrared cameras and specialized markers to track the positions of objects/subjects in three-dimensional space, offering incredibly accurate data for a wide range of applications. To demonstrate the effectiveness of

position tracking and shape reconstruction of the metal sheet comprehensive experiments were conducted.

## 2. Experimental setup

This work aims to track the positions and reconstruct the shape of sheet metal during the English wheeling process. Figure 1 depicts the proposed experimental setup. The proposed system, Vicon, uses 6 infrared cameras to track markers that are placed on the sheet. Because the toolpath occupies a large part of the sheet, markers can only be placed on the outside edges of the sheet to not collide with the wheels while forming. This limits the number of points on the surface for reconstructing the shape of the sheet. One workaround is to place additional markers in the center of the sheet (where the tool path is) after several cycles, capture data with these additional points, and then proceed to remove the markers before starting the next forming cycle. It is worthwhile mentioning that the Vicon system operates by creating local "objects" composed of at least 3 markers. These "objects" must be locally rigid, meaning this small cluster of markers should remain relatively fixed with respect to one another. Otherwise, position-tracking errors will arise. As such clusters of at least 3 markers are put close together. Further details of the components of the system are given next.

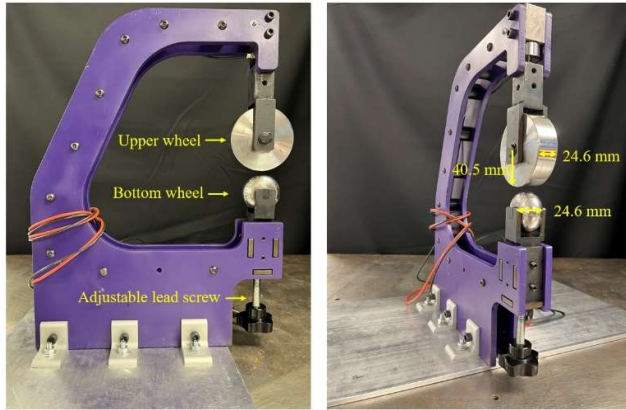


Figure 2. Mini English wheel system designed and made at Northwestern University.

### 2.1. English wheel and robot arm

**English wheel.** The English wheel utilized is shown in Figure 2. It is an Eastwood Elite Mini English Wheel with a 190.5 mm throat with a fully customized frame manufactured in-house. The upper wheel has a lateral radius of 40.5 mm and a frontal width of 24.6 mm. The bottom wheel is doubly curved (lateral and frontal radii) and interchangeable, with a frontal width of 24.6 mm. During this study, a bottom wheel with a frontal radius of 12.7 mm was used.

**Robot arm.** The robot arm (UR5e manufactured by Universal Robot) with an end effector (custom-built gripper) is shown in Figure 3. The custom gripper allows for extra degrees of freedom as the sheet is deforming compared to a static fixed gripper. The gripper has two contact points. Both contact points can rotate. One contact point is laterally fixed, while the other can move laterally along a rail. The custom gripper can conform to the shape of the deforming sheet, which is not possible with a static fixed gripper.

### 2.2. Vicon Motion Capture System

A Vicon motion capture system, equipped with 6 infrared cameras, is utilized. The Vicon system, based on optical tracking, records the three-dimensional movement paths of the reflective markers with an accuracy up to 0.017 mm. The details of the proposed metrology system are illustrated in Figure 1.

**Camera.** The six infrared cameras installed on the setup boast a 1.3 MPX resolution and 330 FPS and excel in swiftly capturing moving subjects, including athletes and drones, or multiple performers/objects, all while maintaining exceptionally low latency. The resolution of the cameras is 1280 × 1024, with a focal length of 4 mm. The field of view (FOV) of each camera is 79.0° (H) × 67.6° (V). The FOV of the whole Vicon system in this work is 1499.8 mm × 1470.1 mm × 628.0 mm (Length × Width × Height).

**Data processing.** The outputs of the Vicon system are the 3D locations of the markers placed on the metal sheet, as depicted

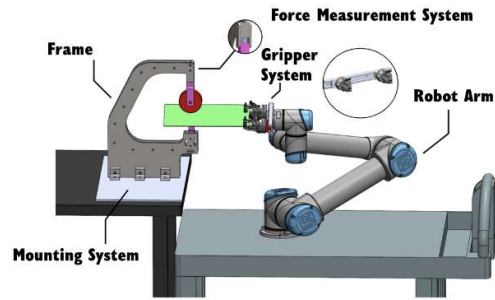


Figure 3. Overview of robot forming components.

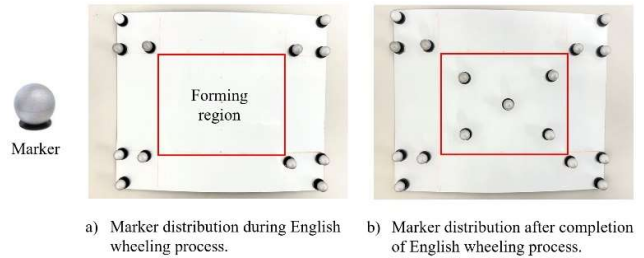


Figure 4. Location of markers during/after the English wheeling process.

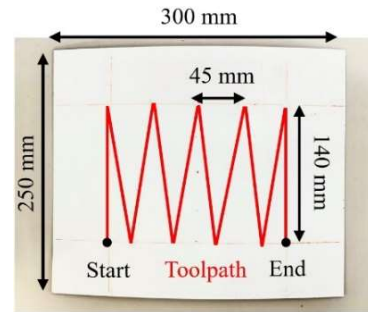


Figure 5. Details of the toolpath and the dimensions of the sheet metal. A cycle encompasses the entire path starting from the initial point (start), going through the red path, and returning to the starting position.

in Figure 4. The markers are machined hemispheres, enveloped in a single layer of 3M's highly reflective materials enhancing spherical precision and facilitating centroid identification even at extended distances and reduced exposure thresholds. By triangulating the reflections of the markers and using the known geometry of the camera setup, Vicon can precisely determine the 3D position of each marker in real-time.

**Accuracy of the Vicon system.** The stated accuracy of the Vicon system in its spec-sheet is 0.017 mm. The accuracy of the entire Vicon system was assessed by placing four pairs of markers at known positions. The system was then tasked with outputting the coordinates, and the discrepancy between the detected distances and the four known lengths used to gauge system accuracy. Ultimately, the accuracy of the proposed system was determined to be 0.11 mm. This error (0.11 mm) also includes the detection error of the Vicon system and the

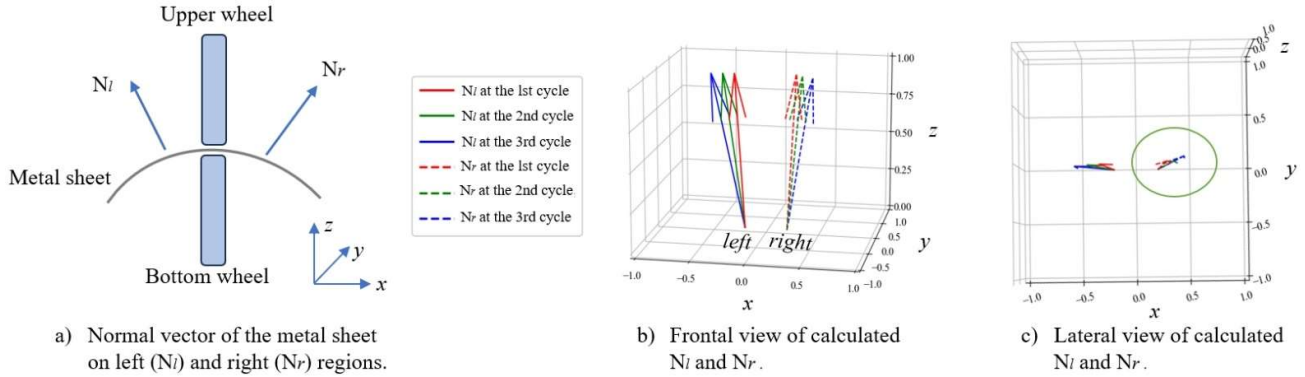


Figure 6. Calculated orientation of two regions on the metal sheet during the English wheeling process.

error from a pre-designed distance (80 mm, 120mm, 160 mm, and 200 mm).

**Metrology method.** The distribution of markers is illustrated in Figure 4. To obtain the positions of the sheet in real time, 3 markers are placed at each corner, as shown in Figure 4(a). In this way, the positions of the sheet can be determined by the Vicon system. There are no markers at the center of the sheet; otherwise, they would be impacted by the wheels during the forming process. To obtain the shape of the metal sheet with high accuracy, five extra markers are placed at the center of the metal sheet after the English wheeling process is finished. Finally, a cubic interpolation method is employed to reconstruct the shape based on the 17 markers shown in Figure 4(b).

### 3. Experiments

To ascertain the proposed system's ability to track the sheet's position (Section 3.1.1) and reconstruct its shape (Section 3.1.2) experiments were conducted on 0.6 mm thick 316L stainless steel sheets along a triangular track pattern/tool path as shown in red in Figure 5. The UR5e robot with the custom gripper was used to move the sheet. Three sheets were wheeled, for 2 cycles, 5 cycles, and 10 cycles, respectively. A cycle is defined as starting at the initial position, reaching the end of the path, and returning to the initial position.

#### 3.1. Position tracking

##### 3.1.1 Curvature

The curvature measurement of the sheet not only provides additional insights into the surface shape but also provides a pathway for future in-situ toolpath updating considering the sheet's deformation. To obtain the curvature of the deformed metal sheet during the process, 12 markers at four corners were used, as depicted in Figure 4(a). However, as pointed out above, it is not possible to stick markers over the entire metal sheet during the deformation process as the markers in the middle of the panel will interfere with the wheeling process. Therefore, two normal vectors ( $N_l$  and  $N_r$ ) are used to represent the curvature of the metal sheet in the left and right regions, respectively, as shown in Figure 6(a). The normal vector for the left region  $N_l$  is computed based on the plane created by the

positions of one left-up marker (Marker A in Figure 4), one left-down marker (Marker B in Figure 4), and one fixed contact point between the wheels and the metal sheet (as seen in Figure 1). The normal vector for the right region  $N_r$  is computed in the same way. To ensure a fair comparison, the normal vectors are computed for both regions when the sheet is at the same position and follows the same movement direction during the first three cycles of the English wheeling process. The outcomes are visually presented in Figures 6(b) and (c). It is evident that: 1) the angle between the normal vector and the  $z$ -axis increases with each successive cycle, and 2) as more cycles are completed, the normal vectors of three cycles are gradually no longer on the same  $xy$ -plane. This observation implies the presence of a twisting phenomenon during the English wheeling process, a phenomenon that aligns with practical expectations in real-world applications.

##### 3.1.2 Movement consistency

The primary objective of this section is to validate the movement consistency of the robot arm and the metal sheet during the English wheeling process, ensuring its repeatability. To this end, three markers are placed on the robot arm to track the robot's movement. To compare the difference in movement between the robot arm and the metal sheet, the rotation and translation matrix of the robot arm position between the initial and the current time step are first computed. Subsequently, these matrices are applied to the initial positions of the 12 markers representing the metal sheet as shown in Figure 4(a). The disparity between the newly transformed positions of the metal sheet and the positions detected by the Vicon system is finally used to represent the level of consistency. Specifically, principal component analysis (PCA) is employed to obtain the rotation matrix  $R$  and translation  $t$  based on the initial positions,  $P_{robot}$ , and current positions,  $P'_{robot}$ , of the robot arm represented by three markers. Singular Value Decomposition (SVD) is applied to perform Principal Component Analysis (PCA) [14], given by:

$$\mu = \frac{1}{N_{robot}} \sum_{i=1}^{N_{robot}} P_{robot(i)},$$

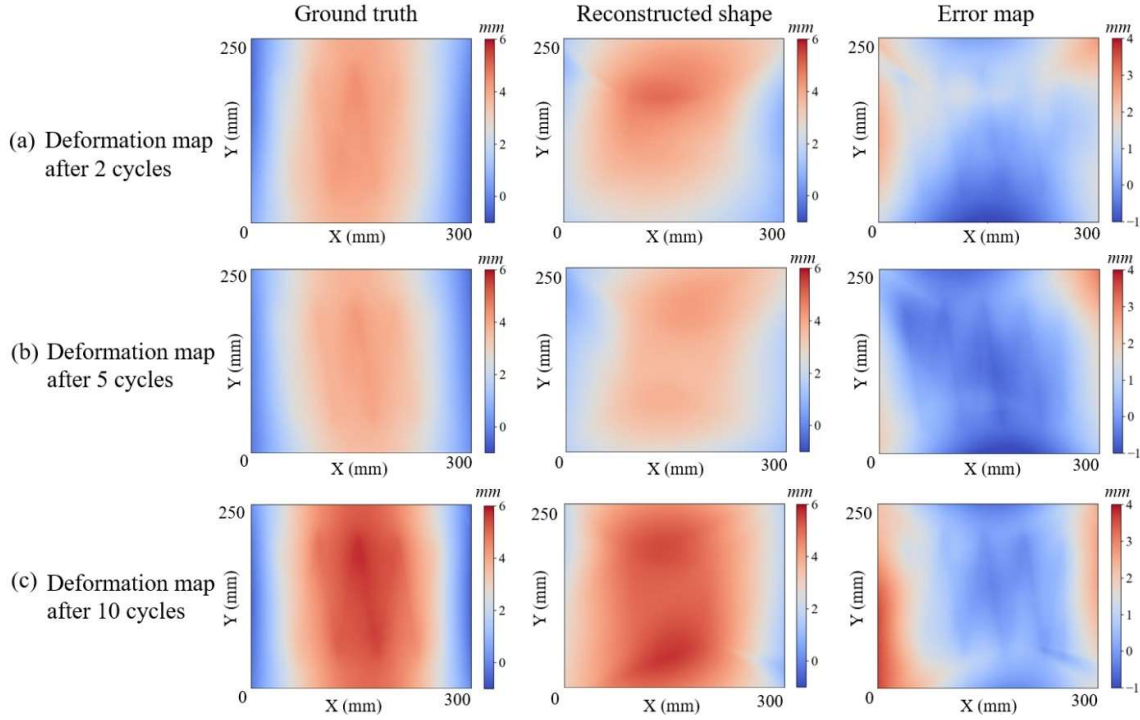


Figure 7. Comparison between the shapes of the metal sheet obtained by the 3D scanner and the reconstructed shape based on the locations of markers.

$$\begin{aligned} \mu' &= \frac{1}{N_{robot}} \sum_{i=1}^{N_{robot}} P'_{robot(i)}, \\ H &= (P_{robot} - \mu)(P'_{robot} - \mu'), \\ [U, S, V] &= SVD(H), \end{aligned} \quad (1)$$

where  $N_{robot}$  represents the number of markers attached to the robot arm, and  $i$  indicates the index of the marker.  $\mu$  and  $\mu'$  are the mean value of marker positions.  $N_{robot}$  is set to 3 in this study.

The rotation matrix,  $R$ , and the translation matrix,  $t$ , of robot arm positions between different time steps can be obtained from:

$$\begin{aligned} R &= VU^T, \\ t &= \mu' - R\mu. \end{aligned} \quad (2)$$

To quantify the difference in movement between the positions of the robot arm and the metal sheet, the Mean Square Error (MSE) is calculated. Specifically, the error is determined by computing the MSE between the current positions of the markers affixed to the metal sheet,  $P'_{sheet}$ , and the transformed initial positions of markers,  $P_{sheet}$ , on the metal sheet. The positions are obtained by the Vicon system. This transformation is achieved using the rotation and translation matrices obtained from the movement of the robot arm.

$$Error = \frac{1}{N_{sheet}} \sum_{i=1}^{N_{sheet}} \|P'_{sheet(i)} - RP_{sheet(i)} - t\|_2, \quad (3)$$

where  $N_{sheet}$  represents the number of markers attached on the metal sheet, and  $i$  indicates the index of the marker.  $N_{sheet}$  is set to 12 in this study.

Based on Eq. 3, the errors are computed during the English wheeling process in two ways: 1) Method A - by evaluating the disparity between the initial positions of the markers on the metal sheet and their subsequent positions, and 2) Method B - by assessing the distinction between two consecutive positions of the markers affixed to the metal sheet. The experimental results are presented in Table 1. The consistency errors calculated through either method are below 1 mm, and the error between two consecutive positions is notably minimal, with a value of 0.12 mm. Considering that the sheet metal is gradually deforming during the English wheeling process, it is reasonable to expect a slightly larger consistency error in Method A (0.60 mm) compared to that in Method B (0.12 mm). In summary, it is deduced that the movement between the robot arm and the metal sheet is remarkably consistent. On the other hand, the movement consistency of the detected robot's movement and the designed toolpath is calculated. The movement of the robot arm is provided by the Vicon system. Based on the collected data, the consistency error between the tracked positions by the Vicon system and the transformed tracked positions, derived from the extracted rotation and translation matrix from the designed path, is 0.21 mm. It should be noted that the path of the markers on the robot arm includes arcs when the robot arm rotates, which is different from the designed toolpath. Therefore, the error in the rotation phase time step is not included.

Table 1. Experimental results of the movement consistency between robot arm and deformed metal sheet.

Method	Details	Error (mm)
Method A	Difference between initial and subsequent time steps	0.60
Method B	Difference between consecutive time steps	0.12

### 3.2. Shape reconstruction

To achieve an accurate surface reconstruction after the English wheeling process, a cubic interpolation method was adopted based on the detected positions provided by the Vicon system. Specifically, seventeen markers were strategically affixed to key locations on the metal sheet, as visually depicted in Figure 4(b). The placement of these markers was thoughtfully considered to ensure comprehensive coverage of the sheet's deformed regions. The Vicon motion capture system was then employed for precise position capture of each of the 17 markers throughout the entire English wheeling procedure. This process yielded a comprehensive dataset, capturing the dynamic spatial coordinates of the markers in real-time. Following the acquisition of marker positions, the surface reconstruction process unfolded. Utilizing a cubic interpolation method, the positions of the 17 markers to seamlessly interpolate and generate a continuous surface representation were leveraged. Incorporating this mathematically precise interpolation method greatly facilitated the estimation of the sheet's shape across its entirety. Employing the cubic interpolation technique, specifically through the determination of coefficients by solving a system of linear equations between adjacent data points, allows for an accurate representation of the surface. In this study, the coefficients were obtained by OpenCV. The choice of cubic interpolation was driven by its ability to maintain smoothness in the data while providing highly accurate estimates of the overall surface shape. This approach enabled continuous and precise estimations across the entire surface.

To assess the accuracy of the reconstructed surface, comparisons with the real shape of the sheet were conducted. The real shape (ground truth) of the deformed metal sheet is obtained by a 7525 Romer Absolute Arm Scanner. The scanned error was within 0.02 mm. It should be noted that while the Vicon system boasts a high accuracy (0.017 mm) in detecting the position of the markers, it is based on the spec-sheet's stated accuracy. The accuracy of the proposed system is 0.11 mm. In contrast, the 7525 Romer Absolute Arm Scanner provides an error specification (0.02 mm) that pertains to the scanning of the entire surface, which is notably lower than 0.11 mm. Therefore, the results obtained by the 7525 Romer Absolute Arm Scanner were taken as the ground truth in this study.

The experimental results are visually depicted in Figure 7. Specifically, three comparisons were conducted to reconstruct the shape of the metal sheet after 2, 5, and 10 cycles of the designed toolpath for the English wheeling process (See Figure 5 for one cycle of the toolpath). Observations from Figure 7 indicate that the general trend of deformation across the entire surface remains consistent, and the primary source of error is

concentrated along the edges of the sheet. Simultaneously, the average error across the entire surface and specifically within the forming regions on the sheet was also computed. The results are listed in Table 2. The average error between the reconstructed shape and ground truth (i.e., the real shape) is around 1 mm for all three experiments, and the average error within the forming regions is notably lower compared to the error across the entire surface. The possible reason for the latter is that the markers are not attached uniformly on the metal sheet, resulting in the reconstructed shape at the edge area having lower accuracy. In summary, the reconstructed shape within the operational regions, based on the precise 3D marker locations detected by the Vicon system, exhibits a notable level of accuracy.

Table 2. Comparison of the reconstructed shape by 3D locations and the ground truth after 2, 5, and 10 cycles of the English wheeling process.

Num. of cycles	Average error (mm)	
	Whole sheet	Forming area
2	0.90	0.52
5	0.69	0.21
10	0.97	0.27

### 3.3. Discussion

In this study, a Vicon motion capture system is employed to track the positions and reconstruct the shape of metal sheets during the English wheeling process. The employed system showed good accuracy but had limitations. "Objects" created through markers (minimum 3) must remain locally non-deformable - otherwise, the detected 3D locations of the markers lose accuracy. To obtain more comprehensive 3D information across the entire metal sheet, additional markers need to be affixed at the center of the sheet after each cycle of the wheeling process is finished.

For more complex surfaces, it is challenging to achieve precise reconstruction solely using Vicon motion capture technology. However, it is crucial to underscore a fundamental strength of the Vicon system: its capability to provide highly accurate 3D point coordinates based on attached markers. Although complex surfaces may pose difficulties for Vicon's reconstruction accuracy, its accuracy in point localization serves as a foundational resource for future endeavors. In future work advanced methodologies, including deep learning techniques, to overcome the limitations associated with reconstructing intricate surfaces will be leveraged. The aim will be to develop a deep learning-based approach to predict the normal vectors across the entire surface and reconstruct the shape of the metal sheet seamlessly. This proposed methodology holds promise for achieving uninterrupted surface reconstruction, addressing a critical need in various applications. Furthermore, the created object based on three markers in Vicon system may cause flipping issues due to the symmetrical shape. Consequently, in future work, more markers will be employed to construct objects, thereby enhancing the robustness of measurements.

On the other hand, while considering the adoption of a plastic deformation model to infer the deformation during the toolpath using markers at the outer edges is a valid proposition, it comes with certain challenges and limitations. Plastic deformation models often require a comprehensive understanding of material properties, complex constitutive equations, and accurate boundary conditions. Moreover, obtaining precise parameters for these models can be challenging. In contrast, the proposed method employs cubic linear interpolation, which offers a balance between computational simplicity and accuracy.

#### 4. Conclusions

This study has delved into the dynamics of the English wheeling process, leveraging advanced metrology techniques, and the Vicon motion capture system, to comprehensively assess and analyze the movement and deformation of the metal sheet. The obtained experimental results underscore the efficacy of the proposed metrology system, showcasing a high level of accuracy in monitoring and reconstructing the shape of the metal sheet. Accurate tracking of sheet deformation can make it feasible to implement updatable robotic toolpaths to better mimic the dexterity of the traditional craftsman.

Future endeavors will focus on addressing inherent system limitations and exploring innovative methodologies, potentially integrating deep learning techniques. The goal is to enhance the system's capabilities, enabling seamless and uninterrupted prediction of metal sheet orientation and shape. This continuous evolution at the intersection of traditional craftsmanship and cutting-edge technology holds promising prospects for advancing the field of metalworking, paving the way for more efficient and accurate practices.

#### Acknowledgments

This research was supported by the National Science Foundation under Grant Number CNS-2229170, and CNS-2328032. The authors would also like to acknowledge support from the NSF Engineering Research Center for Hybrid Autonomous Manufacturing Moving from Evolution to Revolution (ERC-HAMMER) under Award Number EEC-2133630.

#### References

- [1] Schuh, G., Bergweiler, G., Fiedler, F., Bickendorf, P., & Colag, C. (2019, December). A review on flexible forming of sheet metal parts. In 2019 IEEE International Conference on Industrial Engineering and Engineering Management (IEEM) (pp. 1221-1225). IEEE.
- [2] Abd El-Aty, A., Guo, X., Lee, M. G., Tao, J., Hou, Y., Hu, S., Li, T., Wu, C., & Yang, Q. (2023). A review on flexibility of free bending forming technology for manufacturing thin-walled complex-shaped metallic tubes. *International Journal of Lightweight Materials and Manufacture*, 6(2), 165-188.
- [3] Bowen, D. T., Russo, I. M., Cleaver, C. J., Allwood, J. M., & Loukaides, E. G. (2022). From art to part: Learning from the traditional smith in developing flexible sheet metal forming processes. *Journal of Materials Processing Technology*, 299, 117337. [4] Huang, D., Suarez, D., Kang, P., Ehmann, K., & Cao, J. (2023). Robot forming: Automated English wheel as an avenue for flexibility and repeatability. *Manufacturing Letters*, 35, 342-349.
- [5] Vermeulen, M. M. P. A., Rosielle, P. C. J. N., & Schellekens, P. H. J. (1998). Design of a high-precision 3D-coordinate measuring machine. *Cirp Annals*, 47(1), 447-450.
- [6] Ju, Y., Shi, B., Jian, M., Qi, L., Dong, J., & Lam, K. M. (2022). Normattention-psn: A high-frequency region enhanced photometric stereo network with normalized attention. *International Journal of Computer Vision*, 130(12), 3014-3034.
- [7] Li, M., Zhou, Z., Wu, Z., Shi, B., Diao, C., & Tan, P. (2020). Multi-view photometric stereo: A robust solution and benchmark dataset for spatially varying isotropic materials. *IEEE Transactions on Image Processing*, 29, 4159-4173.
- [8] Edl, M. M. T. J., Mizerák, M., & Trojan, J. (2018). 3D laser scanners: history and applications. *Acta Simulatio*, 4(4), 1-5.
- [9] Marattukalam, J. J., Karlsson, D., Pacheco, V., Beran, P., Wiklund, U., Jansson, U., ... & Sahlberg, M. (2020). The effect of laser scanning strategies on texture, mechanical properties, and site-specific grain orientation in selective laser melted 316L SS. *Materials & Design*, 193, 108852.
- [10] Yang, H., Omidalizarandi, M., Xu, X., & Neumann, I. (2017). Terrestrial laser scanning technology for deformation monitoring and surface modeling of arch structures. *Composite Structures*, 169, 173-179.
- [11] Xu, X., Yang, H., Augello, R., & Carrera, E. (2021). Optimized free-form surface modeling of point clouds from laser-based measurement. *Mechanics of Advanced Materials and Structures*, 28(15), 1570-1578.
- [12] Furtado, J. S., Liu, H. H., Lai, G., Lacheray, H., & Souza-Coelho, J. (2019). Comparative analysis of optitrack motion capture systems. In *Advances in Motion Sensing and Control for Robotic Applications: Selected Papers from the Symposium on Mechatronics, Robotics, and Control (SMRC'18)-CSME International Congress 2018, May 27-30, 2018 Toronto, Canada* (pp. 15-31). Springer International Publishing.
- [13] Sharma, S., Verma, S., Kumar, M., & Sharma, L. (2019, February). Use of motion capture in 3D animation: motion capture systems, challenges, and recent trends. In 2019 international conference on machine learning, big data, cloud and parallel computing (comitcon) (pp. 289-294). IEEE.
- [14] Wall, M. E., Rechtsteiner, A., & Rocha, L. M. (2003). Singular value decomposition and principal component analysis. In *A practical approach to microarray data analysis* (pp. 91-109). Boston, MA: Springer US.